Croatian Society for Materials Protection

Metalurgija/Metallurgy

Vol. 66 No. 1 / 2027

Anti-corrosion Behaviour of an Epoxy Resin Coating Modified with Hydrophobic Nano-silica on a Q235 Carbon Steel Surface

Yan Lv[1,2*] and Xin-yu Pan[3]

https://doi.org/10.64486/m.66.1.7

[1] School of New Materials and Chemical Engineering, Tangshan University, Hebei Tangshan 063000, China
[2] Tangshan Key Laboratory of Chemical Environmental protection and New Film coating Materials, Hebei Tangshan 063000, China
[3] College of E-commerce, Tangshan University, Hebei Tangshan 063000, China
* Correspondence: lvyan@tju.edu.cn

Type of the Paper: Article
Received: February 12, 2026
Accepted: May 12, 2026

Abstract: Corrosion poses pervasive threats to daily-life infrastructure, causing severe economic losses and potential safety hazards, which underscores the urgent demand for high-performance anti-corrosion coatings. This study focuses on enhancing the corrosion resistance and service reliability of phosphated Q235 carbon steel by developing an epoxy coating modified with hydrophobic nano-silica, thereby contributing to the reduction of corrosion-induced risks and potential economic losses in practical applications. The coatings were systematically characterized using scanning electron microscopy, static contact angle measurements, thermogravimetric analysis, and electrochemical techniques. The results demonstrate that the nano-silica-doped coating significantly improves the corrosion protection performance, thermal stability, and surface hydrophobicity of phosphated Q235 steel, with the water contact angle increasing at higher nano-silica loadings. This work confirms that hydrophobic nano-silica modification represents an effective strategy to optimize epoxy anti-corrosion coatings, which is beneficial for prolonging service life and improving the operational safety of carbon steel components in service environments.

Keywords: hydrophobic; nano-silica; epoxy; coating; corrosion

1. Introduction

In the 21st century, with the integration of knowledge and technology across disciplines, new scientific and technological advancements continuously emerge, and the innovation in functional materials progresses. Among these, hydrophobic materials have gained attention and become a prominent research topic. Hydrophobic materials exhibit significant application prospects in metal corrosion protection, self-cleaning, fluid drag reduction, and other domains. Their role in corrosion protection is particularly crucial for national economic sustainability. Corrosion of metallic materials refers to the phenomenon wherein materials undergo electrochemical or chemical reactions with surrounding substances to form metallic compounds. Corrosion problems exist in many areas, such as storage tank surfaces, oil pipelines, and ship hulls. Such degradation can lead to pipeline rupture, increased drag resistance of vessels, and incalculable economic losses. Approximately 100 million tons of metal are scrapped annually due to corrosion. Globally, resultant economic losses account for 3.5 %–4.2 % of gross domestic product (GDP), exceeding losses from natural disasters

https://doi.org/10.64486/m.66.1.7

including floods, droughts, earthquakes, and tsunamis. In addition, corrosion can lead to environmental pollution, causing degradation and shortages of land and water resources [1].

As one of the commonly employed methods for corrosion mitigation, organic coatings can serve as a physical barrier that isolates the metal substrate from water, dissolved oxygen, and corrosive ions, thereby reducing metal corrosion [2]. Consequently, developing corrosion-resistant functional materials holds significant importance.

Epoxy, as a common polymer material, has excellent adhesive properties and can effectively bond with both metallic and non-metallic materials. It is widely used in industries such as coating and packaging, especially in waterproof coating, where it is more commonly applied [3]. Although epoxy can be directly used as a coating material to act as a physical barrier to prevent the entry of harmful substances, epoxy alone is not sufficient. It also has many disadvantages and certain limitations. For instance, epoxy itself is relatively brittle, and its performance is not up to standard in some parts of the material that require resistance to fracture. During the curing process of epoxy, voids are formed. The presence of these voids enables the intrusion of oxygen, water, and corrosive ions (like chloride ions and hydrogen ions) into the coating. After these corrosive species enter the coating, they undergo electrochemical reactions with the metal substrate, causing blisters and accumulation of corrosive species, thereby accelerating the corrosion process. This greatly shortens the lifespan of the coating and leads to a substantial rise in maintenance expenses. Embedding corrosion-resistant materials into the gaps within the epoxy coating can markedly improve its resistance to corrosion [4,5].

Fillers obstruct micropores and cavities within the coating matrix, thereby decreasing the diffusion of electrolytes to the interface between the coating and metal. Adding fillers reduces coating defects and lengthens water diffusion paths, enhancing corrosion resistance [6]. Nano-silica particles are frequently employed as fillers in conventional organic coatings. Known as a promising polymer-based hybrid material, nano-silica features adjustable dimensions, thermal stability, chemical resistance, and outstanding reinforcement characteristics. Grari et al. [7] used a layering technique to incorporate nano-silica powder into a polypyrrole matrix. The composite coating comprises two layers: electrochemically grown polypyrrole and electrophoretically deposited silica particles. In contrast to direct mixing, the layer-by-layer approach demonstrates superior performance in integrating nano-silica particles, which enhances the material's corrosion resistance. Shi et al. [8] developed SiO_2/ PANI (polyaniline) nanocomposites through the growth of silica spheres within a polyaniline solution, effectively enclosing the nano-silica particles within polyaniline coatings. These nanocomposites were mixed with organosilicon to form an organosilicon-SiO_2 / PANI (polyaniline) composite coating, which demonstrates exceptional water-repellent properties and remarkable resistance to permeation. Peres et al. [9] found that incorporating nano-silica nanoparticles enhances the anti-corrosion capabilities of polysiloxane coatings.

Hydrophobic surfaces provide corrosion protection by impeding water and corrosive ion transfer [10]. For example, in atmospheric environments, their microstructure traps air, reducing water droplet contact area. Researchers hypothesize that hydrophobic coatings inhibit atmospheric corrosion by hindering electrolyte film formation [11]. The air film also acts as a self-cleaning barrier, preventing water droplets and dissolved ions from adhering. This effect enhances corrosion protection in rainy conditions [12]. In immersed environments, the air film forms a temporary barrier, isolating the substrate from corrosive surroundings. Liu et al. [13] demonstrated a superhydrophobic fluoropolymer coating on zinc, exhibiting 29 days of corrosion resistance in 3.0 wt.% NaCl solution. Zhang et al. [14] utilized a superhydrophobic coating on titanium, extending its corrosion resistance to 90 days. In addition, hydrophobic surfaces can be fabricated via methods such as platinum displacement, octadecyltrimethoxysilane self-assembly, polythiophene electrodeposition, spraying of metal salt-alkyl thiol reaction products, stearic or myristic acid modification, and impregnated polypropylene-fluoroalkyl silane self-assembly [15]. Overall, corrosion resistance stems from air layers trapped in surface valleys, decreasing water contact area and blocking corrosive media. Thus, metals with hydrophobic surfaces show improved corrosion resistance. Furthermore, these surfaces exhibit anti-fouling

https://doi.org/10.64486/m.66.1.7

properties against dust, graphite powder, alumina powder, calcium carbonate, and calcium sulfate fouling, with the air layer preventing dirt particle transfer.

Epoxy resin coatings are widely used for metal corrosion protection in aqueous electrolyte environments, but moisture penetration can degrade their performance. Enhancing water resistance can delay the penetration of corrosive solutions and improve durability. This work innovatively embedded hydrophobic silica nanoparticles into epoxy resin coatings and applied them to phosphorized Q235 carbon steel surfaces. The effects of regulating the doping amount of hydrophobic nano-silica on the microstructure, thermal stability, hydrophobicity and anticorrosion performance of epoxy coatings were systematically investigated, aiming to validate the role of hydrophobic nano-silica in effectively enhancing the hydrophobicity, thermal stability, and anti-corrosion performance of epoxy resin coatings.

2. Experimental Instruments and Materials

2.1 Experimental Apparatus

Magnetic stirrer, 90-4; Ultrasonic cleaner, JK-5200B; Scanning electron microscope, SU8010; Contact angle measuring instrument, OCA20; Thermogravimetric analyzer, Q500.

2.2 Experimental Materials

Q235 carbon steel; Trihydroxymethylpropane triglycidyl ether, analytically pure; Diethylidene triamine, analytically pure; hydrophobic nano-silica, analytical grade; Anhydrous ethanol, analytically pure; Graphite electrode, Beijing Jinglongte Carbon Graphite Plant.

3. Experiment process

3.1 Synthesis of Traditional Epoxy Coating

100.0 g trihydroxymethylpropane triglycidyl ether and 18.6 g diethylenetriamine were mixed and stirred for 30 minutes at room temperature to obtain a low-viscosity prepolymer mixture. Subsequently, using a pipette, 5.0 mL of the mixture was dispensed onto the surface of the phosphated carbon steel substrate (100 mm×200 mm×2 mm), where it was uniformly spread. After curing at 80 °C for 60 min, a conventional epoxy coating was formed.

Figure 1 shows the chemical reaction equation of epoxy polymerization which occurs between trihydroxymethylpropane triglycidyl ether and diethylenetriamine. After cross-linking, a solid and hard epoxy coating is formed [16].

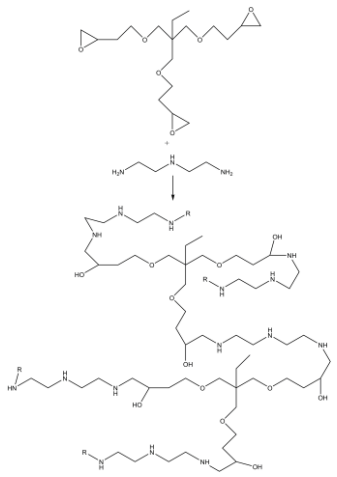

Figure 1. The chemical reaction equation of traditional epoxy polymerization [16]

https://doi.org/10.64486/m.66.1.7

3.2 Synthesis of Epoxy Coating Modified with Hydrophobic Silica Nanoparticles

Figure 2 illustrates the synthesis of the epoxy coating modified with hydrophobic silica nanoparticles. First, 100.0 g trihydroxymethylpropane triglycidyl ether and a certain amount (see Table 1) of hydrophobic silica nanoparticles were physically blended by mixing and stirring at room temperature for 30 minutes to obtain nanoparticle mixture A. Then, nanoparticle mixture A was mixed with the 18.6 g diethylenetriamine curing agent to obtain nanoparticle prepolymer mixture B. Subsequently, the mixed solution was dispensed onto the surface of the carbon steel substrate with a pipette and uniformly spread across it. Finally, the carbon steel sample coated with nanoparticle prepolymer mixture B was placed at 80 °C for 60 minutes, resulting in a carbon steel sample coated with a hydrophobic nano-silica modified epoxy coating. The dry film thickness of the nano-silica modified epoxy coating is about 100 μm.

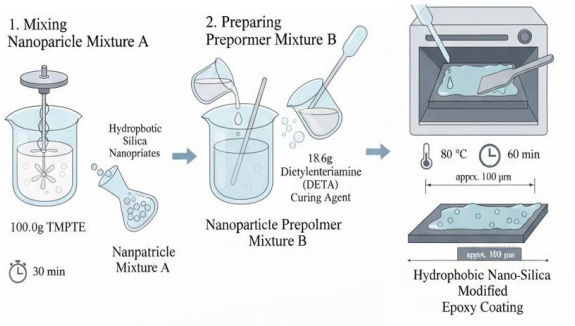

Figure 2. Schematic illustration of the synthesis of the epoxy coating modified with hydrophobic silica nanoparticles

3.3 Preparation of carbon steel samples coated with traditional epoxy coating

Absolute ethanol (5 g) was transferred to a beaker using a disposable dropper. Trimethylolpropane triglycidyl ether (4.148 g) and diethylenetriamine (0.852 g) were added sequentially. The solution was mixed on a magnetic stirrer for 10 minutes. Subsequently, a pipette was used to apply the solution uniformly onto the phosphated carbon steel sample, with an applied volume of 300 μL. The coated sample was left at room temperature for 10 minutes to partially evaporate the solvent, increasing the coating viscosity. It was subsequently cured in a drying oven at 80 °C for (30–60) minutes to accelerate solvent evaporation and promote coating curing. The resulting carbon steel sample, designated TES, was coated with a traditional epoxy coating.

3.4 Preparation of carbon steel samples with epoxy coating incorporating hydrophobic silica nanoparticles

Hydrophobic silica (0.3 g) was weighed with an electronic balance into a beaker, then anhydrous ethanol (4.85 g) and trihydroxymethylpropane triglycidyl ether (4.024 g) were added, followed by diethylenetriamine (0.826 g). The mixture was placed on a magnetic stirrer for 10 min. The phosphated carbon steel sample was uniformly covered with the mixture using a pipette, applying 300 μL of the coating solution. After coating with the prepolymer mixture, the carbon steel sample was left undisturbed at room temperature for 10 minutes. It was subsequently transferred to a drying oven and subjected to heat treatment at 80 °C for (30–60) min. The MES1 carbon steel sample was coated with a hydrophobic nano-silica-doped epoxy resin coating. The modified epoxy coatings of MES2, MES3, and MES4 were then prepared in a similar way. The composition ratios of MES2, MES3, and MES4 are shown in Table 1.

Table 1. Composition ratio of hydrophobic nano-silica-modified epoxy anti-corrosion coatings

	TES/g	MES1/g	MES2/g	MES3/g	MES4/g
Trihydroxymethylpropane triglycidyl ether	4.148	4.024	3.941	3.816	3.734
Diethylenetriamine	0.852	0.826	0.809	0.784	0.766
Absolute ethanol	5	4.85	4.75	4.6	4.5
Hydrophobic nano-silica	0	0.3	0.5	0.8	1

https://doi.org/10.64486/m.66.1.7

4. Results and Discussion

4.1 Characterization test and corrosion analysis of hydrophobic nano-silica modified epoxy coating

4.1.1 Scanning electron microscopy (SEM) characterization test

Figure 3 shows the microscopic morphology of the hydrophobic nano-silica-modified epoxy coating. Figure 3 (a) shows that there are no particles on the coating surface, indicating that it is complete and even. Figure 3 (b) displays a small amount of aggregates on the MES1 surface. Increasing nano-silica content leads to more aggregates on the modified epoxy coating, as shown in Figures 3 (c), (d), and (e). The aggregates have a diameter of approximately 5 μm. As the amount of nano-silica added increases, the coating surface becomes increasingly dense. These aggregates can effectively delay the diffusion of corrosion media.

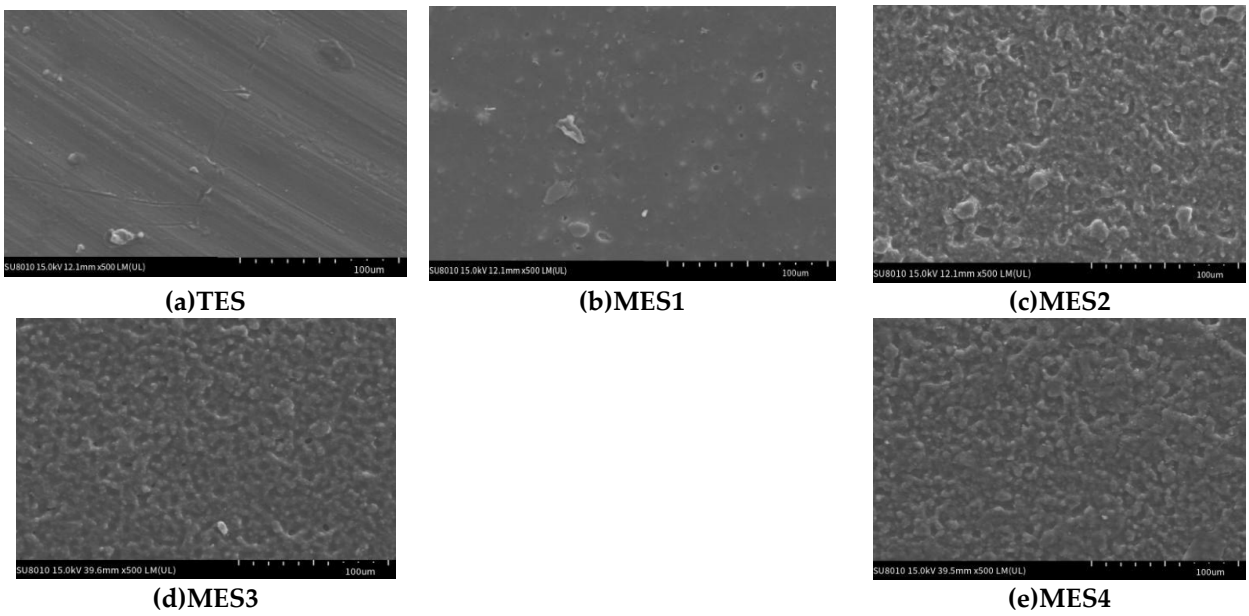

Figure 3. Microscopic Appearance of TES(a), MES1(b), MES2(c), MES3(d), and MES4(e)

4.1.2 Thermogravimetric analysis

Figure 4 illustrates the thermal stability of the modified epoxy coatings, as all samples maintain roughly 97 % of their weight at 250 °C. At temperatures exceeding 250 °C, there is a notable decrease in the weight of all coatings, suggesting that the modified epoxy coatings start to break down at higher temperatures. When the temperature is below 350 °C, the three coatings MES1, MES2, and MES3 exhibit similar trends of residual weight variation. When the temperature exceeds 400 °C, the weights of MES1, MES2, and MES3 vary. Epoxy coatings with various modifications incorporate different levels of nano-silica. At 450 °C, the residual weights of MES1, MES2, and MES3 are approximately 14 %, 16 %, and 27 %, respectively. Above 450 °C, the weight change trend becomes nearly flat, indicating complete decomposition of the organic component. Compared with MES1 and MES2, MES3 contains the most nano-silica and has a higher decomposition temperature. Therefore, MES3 has better thermal stability due to the higher content of nano-silica incorporated in MES3 compared to that in MES1 and MES2. With the increase of the content of nano-silica, the crosslinking degree of the residual Si-OH with the matrix resin is greater, and the binding with the phosphorized carbon steel surface is stronger, which makes the coating denser and firmer, and thus improves the thermal stability. It can be concluded that the thermal stability of epoxy coatings can be improved effectively by adding nano-silica.

https://doi.org/10.64486/m.66.1.7

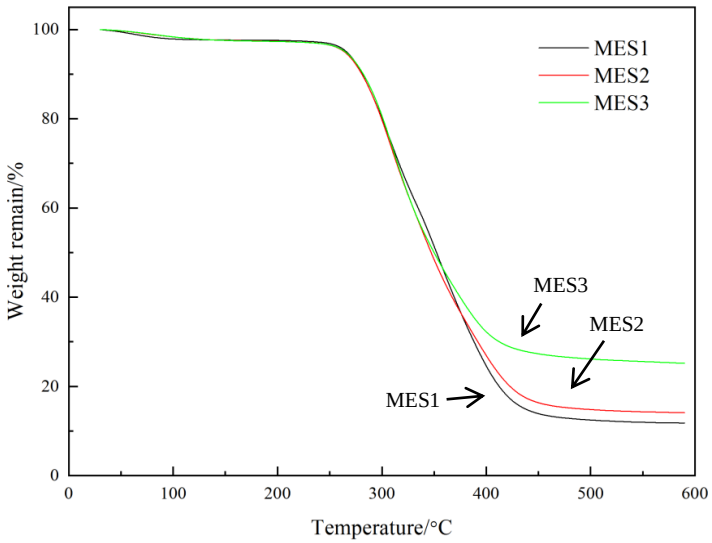

Figure 4. Thermal stability of various modified epoxy coating

4.1.3 Static contact angle measurements

Figure 5 shows the water contact angles of different epoxy coatings. In contrast to TES, the incorporation of hydrophobic nano-silica considerably improves the hydrophobic properties of conventional epoxy coatings. The average contact angles are approximately 66.7° for TES, 83.2° for MES1, 83.4° for MES2, 81.3° for MES3, and 95.9° for MES4. MES4, containing hydrophobic nano-silica, exhibits the highest hydrophobicity and is hydrophobic with a contact angle exceeding 90°.

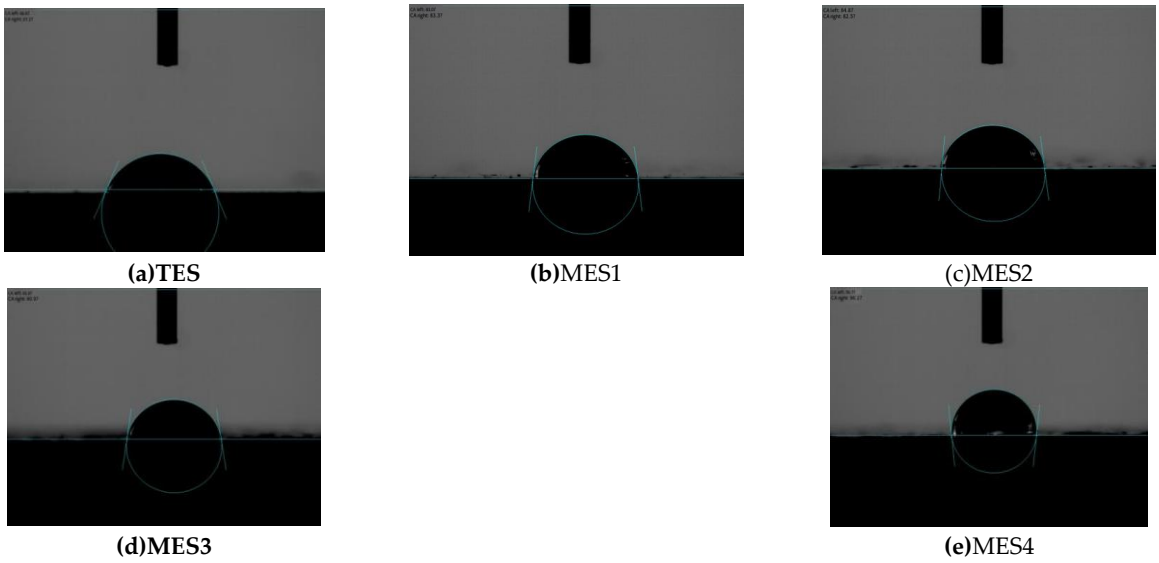

Figure 5. Static Contact Angles of 3 μL Water Droplets on the Surfaces of TES (a), MES1 (b), MES2 (c), MES3 (d), and MES4 (e)

4.1.4 Electrochemical characterization analysis

In order to investigate the corrosion behavior, all samples were immersed in a 3.5 wt.% NaCl aqueous solution for varying durations. Figure 6 presents the OCP (open-circuit potential) values of the different samples immersed in the 3.5 wt.% NaCl solution over time. The OCP value is influenced by the anodic and cathodic reactions occurring in the solution as well as the resistance of the electrolyte. During the initial

https://doi.org/10.64486/m.66.1.7

immersion phase, all samples demonstrated relatively high OCP values. A higher OCP value suggests that the coating possesses effective initial barrier properties [17]. Specifically, the initial OCP values for TES, MES1, MES2, MES3, and MES4 were approximately -0.3979 V, -0.2391 V, -0.2375 V, -0.2947 V, and -0.2637 V, respectively. However, as the immersion time increased, the OCP value dropped rapidly, indicating that the corrosion medium penetrated the coating, resulting in an increase in the coating's capacitance. After immersion for 6 h, the OCP values of TES, MES1, MES2, MES3 and MES4 decreased to about −0.5092 V, −0.5379 V, −0.5271 V, −0.3567 V and −0.3354 V, respectively. The OCP value of the MES4-coated sample decreased more slowly than those of the other coatings, demonstrating superior corrosion resistance. The reason is that with the increase of silica content, the compactness of the coating is improved, making it more difficult for corrosive medium to penetrate to the carbon steel surface. The corrosion reaction is effectively inhibited, and the electrode system becomes more stable. Therefore, the open-circuit potential (OCP) shifts positively and increases. The OCP value for pure carbon steel in NaCl solution is approximately −0.6 V. After approximately 30 hours of soaking, TES, MES1, MES2, and MES3 reached about −0.6 V, signifying substrate corrosion. However, MES4 reached this value after about 300 hours, indicating corrosion onset only after prolonged exposure.

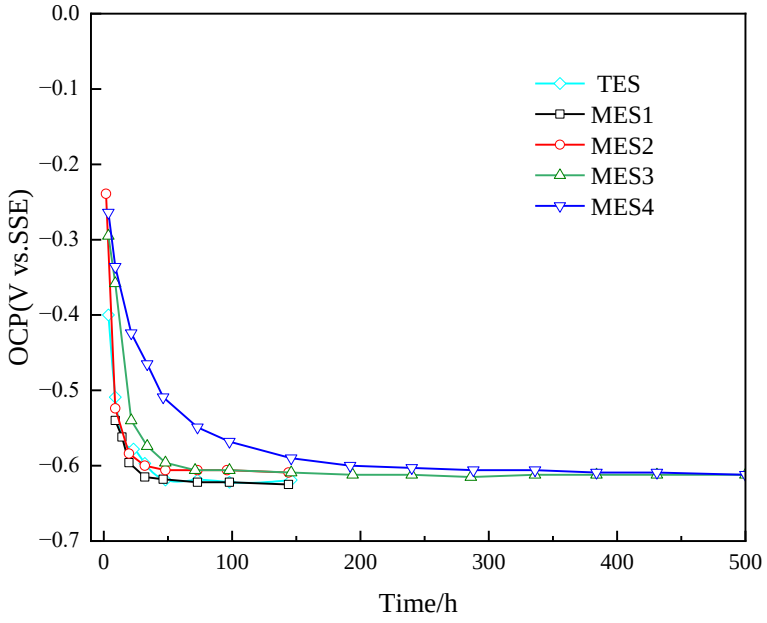

Figure 6. OCP values of TES, MES1, MES2, MES3, and MES4 samples immersed in 3.5 wt.% NaCl solution for different immersion times

Electrochemical impedance spectroscopy is used to evaluate the corrosion resistance of various coatings. Figure 7 presents the Bode impedance plots for Q235 carbon steel samples coated with TES, MES1, MES2, MES3, and MES4. As seen in Figure 7, all MES-coated samples exhibit high impedance, indicating that nano-silica addition enhances traditional epoxy corrosion resistance. Impedance rises with increasing nano-silica content. This improvement may stem from nanoparticles extending the diffusion path of corrosion medium. Higher nanoparticle concentrations lead to longer, more complex diffusion paths [17]. When the hydrophobic nano-silica content reaches approximately 8 wt.% or higher, the anti-corrosion performance improves significantly, as shown by MES3's curve in Figure 7. Additionally, MES4 coating, with the highest nanoparticle concentration, shows the highest impedance. Enhanced hydrophobicity further delays water and dissolved ion penetration.

https://doi.org/10.64486/m.66.1.7

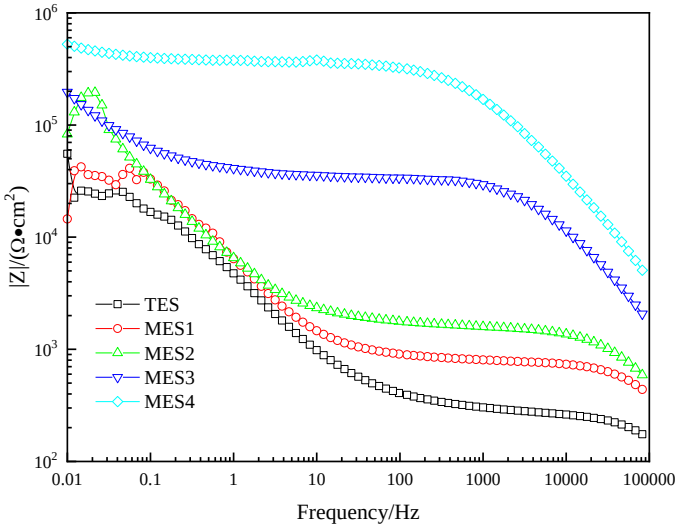

Figure 7. Bode impedance plots of Q235 carbon steel samples coated with TES, MES1, MES2, MES3, and MES4

Figure 8 shows the impedance changes of samples with different coatings of TES, MES1, MES2, MES3 and MES4 at different immersion times. It indicates that as the concentration of hydrophobic nano-silica nanoparticles rises, the material's corrosion resistance improves. It is widely recognized that AC impedance in the low-frequency range is effective for evaluating the barrier properties of a coating [18]. Consequently, a coating with higher impedance exhibits superior anti-corrosion capabilities. It can be seen from Figure 8 that the impedance of different samples immersed for 143 h at 0.01 Hz frequency is 185 Ω·cm² (TES), 100 Ω·cm² (MES1), 328 Ω·cm² (MES2) and 4092 Ω·cm² (MES3), respectively. All immersed samples exhibit impedance values significantly higher than carbon steel, approximately 22 Ω·cm² at 0.01 Hz. Figure 8(a) shows an impedance increase after 70 hours of immersion in 3.5 wt.% NaCl solution. This increase may result from corrosion products on the carbon steel matrix. These corrosion products act as a barrier against corrosion media penetration [18]. Figure 8(e) indicates that MES4 reaches a maximum impedance of 4.51×10⁴ Ω·cm² after 143 hours at 0.01 Hz, where corrosion resistance is optimal. Comparing impedance values of MES3 and MES4 with TES, MES1, and MES2 reveals that anti-corrosion performance improves significantly above a threshold nano-silica content.

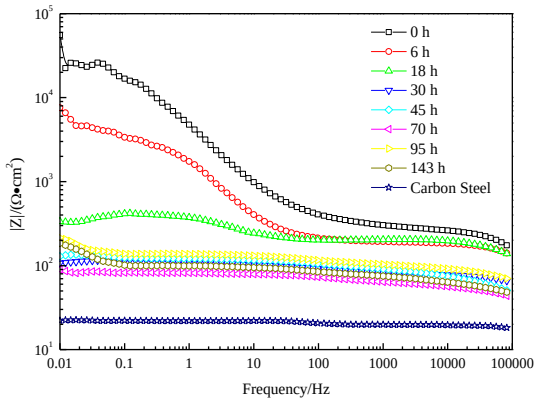

(a) TES

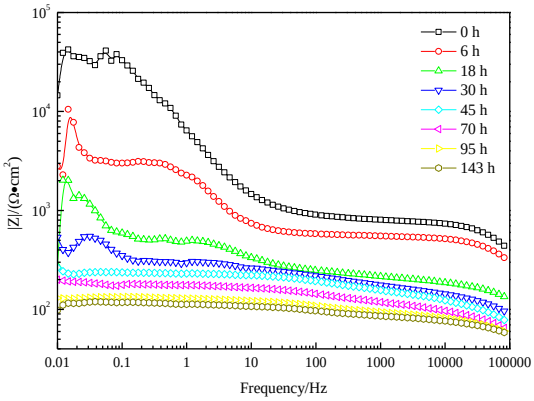

(b) MES1

https://doi.org/10.64486/m.66.1.7

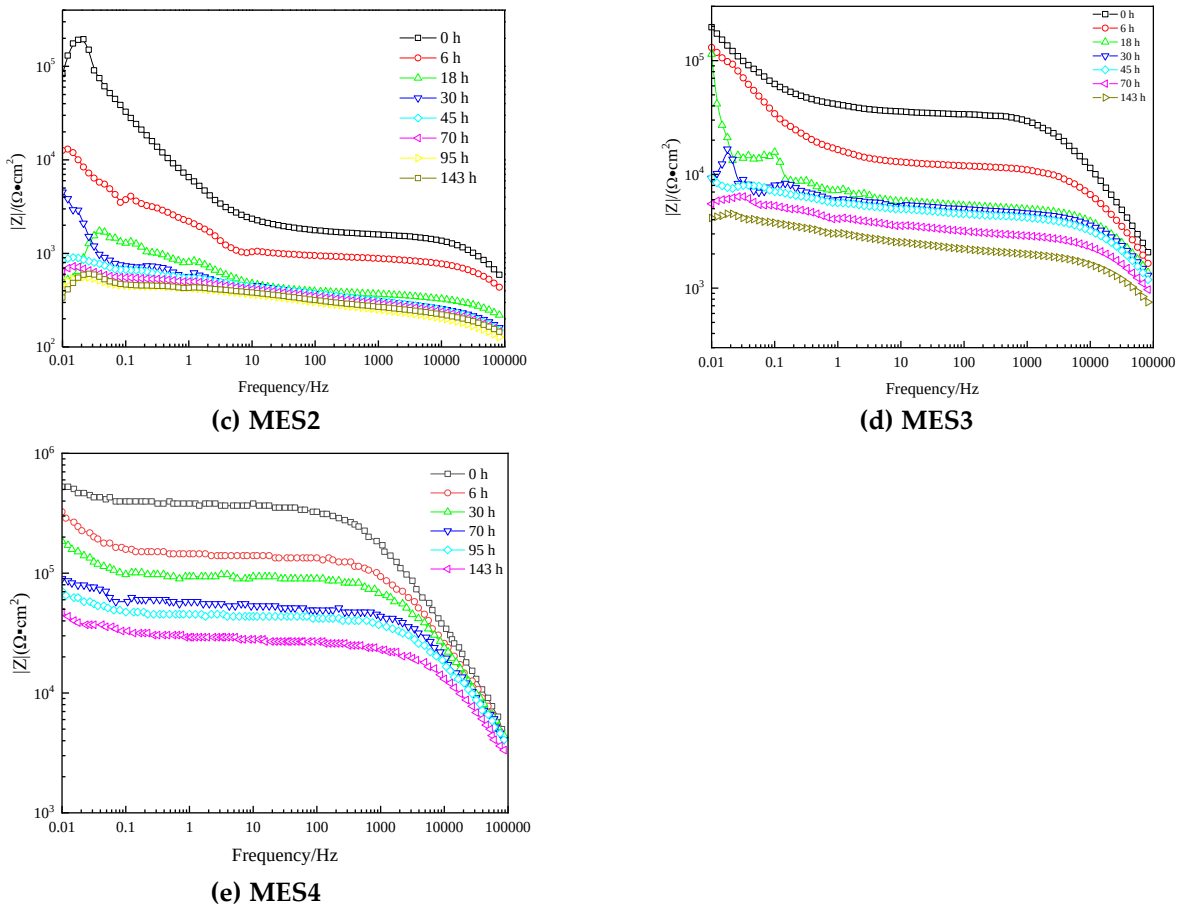

Figure 8. The Bode impedance diagrams of the coating samples TES (a), MES1 (b), MES2 (c), MES3 (d) and MES4 (e) at different immersion times

The Bode diagrams are shown in Figure 9, where the area under the impedance frequency curve divides into resistance and capacitance regions. Regions with phase angles above and below 45° correspond to capacitance and resistance regions, respectively. The low-frequency resistance region indicates coating delamination. A decrease in the capacitance region implies that the electrolyte has penetrated into the substrate as a result of coating deterioration [19]. In Figure 9(a), two separate areas can be observed: a low-frequency resistance area and a high-frequency capacitance area. Following 95 hours of immersion, as shown in Figure 9(b), there is an expansion of the resistance area alongside a reduction in the capacitance area, which suggests the diffusion of corrosive substances, separation of the coating, and diminished adhesion. The Coating Damage Index (CDI) reflects coating integrity. CDI can be calculated as follows:

$$CDI = \frac{A_2}{A_1} \tag{1}$$

In the formula, A1 and A2 represent the integrated areas of the capacitance and resistance regions, respectively. After initial immersion in 3.5 wt.% NaCl solution, the CDI of MES4 was 0.165. After 95 h of immersion, the CDI increased to 0.415. This indicates an expansion in the corrosion damage range.

https://doi.org/10.64486/m.66.1.7

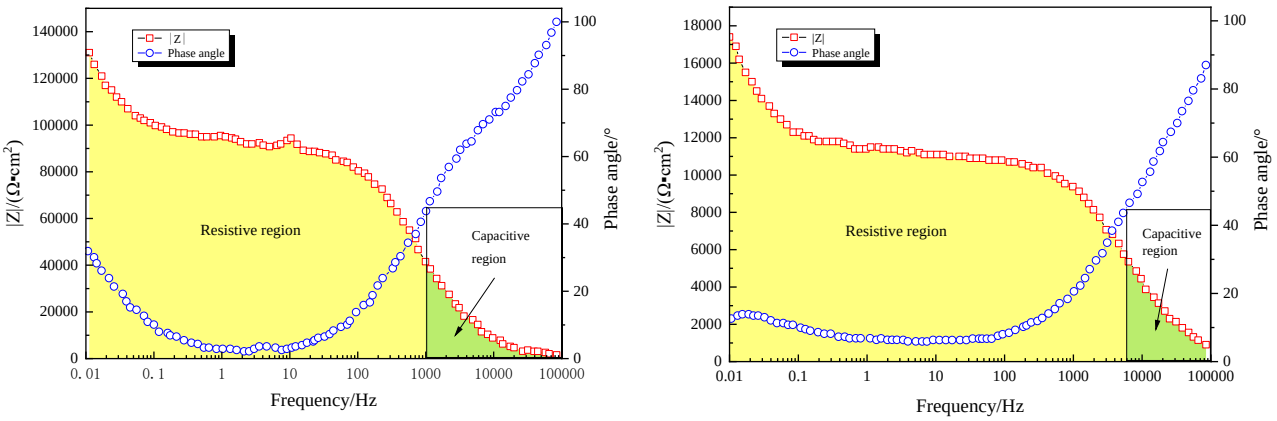

Figure 9. Bode plots of MES4 immersed in 3.5 wt.% NaCl solution for 0 h (a) and 95 h (b)

In order to investigate the corrosion behavior of MES4-coated Q235 carbon steel samples, equivalent circuit simulation was employed. Figure 10 displays the phase angle diagram for MES4, revealing two characteristic peaks that suggest two state variables in the surface corrosion reaction during the electrode process. Therefore, the equivalent circuit $R_s(QR_c)c(QR_{dl})_{ct}$, which incorporates two state variables, was utilized to simulate the electrochemical impedance spectrum of carbon steel coated with MES4. Here, R_s represents the solution resistance, Q_c stands for the coating capacitance impedance, R_c is the coating resistance, Q_{dl} indicates the double-layer capacitance impedance, and R_{ct} corresponds to the charge transfer resistance. Owing to dispersion effects in electrochemical processes, the constant phase angle element Q replaced the pure capacitor C to represent impedance from coating and double-layer capacitances. The impedance of Q is expressed as $Z_Q = 1/Y_0 \bullet (j\omega)^{-n}$. In this context, ω represents the angular frequency of the AC electrical signal applied through an electrochemical workstation, while n denotes the dispersion coefficient. A value of n equal to 0 or 1 indicates that the constant phase angle element is equivalent to either pure resistance or pure capacitance [19]. Figure 11 presents the equivalent circuit used for fitting the electrochemical impedance spectrum of Q235 carbon steel coated with MES4 in a 3.5 wt.% NaCl solution.

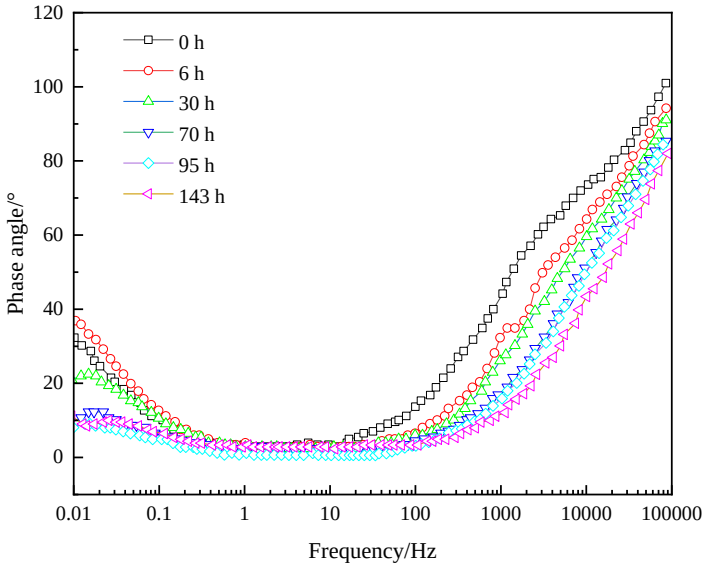

Figure 10. Bode phase angle diagram of MES4

https://doi.org/10.64486/m.66.1.7

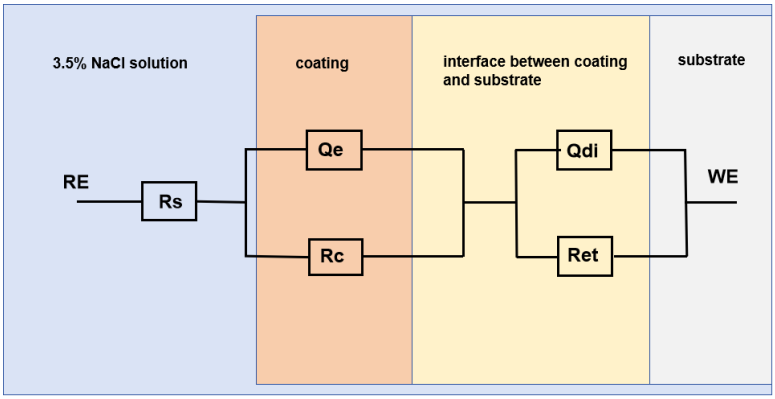

Figure 11. Impedance fitting equivalent circuit of Q235 carbon steel coated MES4 in 3.5 wt.% NaCl aqueous solution

Furthermore, the volume fraction of water absorbed in the coating, χ_V, can be calculated using the Brasher–Kingsbury equation [20]:

$$\chi_V = \frac{\log \frac{Y_{0,t}}{Y_0}}{\log \varepsilon_w} \tag{2}$$

$Y_{0,t}$ is a parameter of a constant phase angle element Q_c with immersion time t whose impedance is equal to $Z_{Qc} = 1/Y_{0,t} \bullet (j\omega)^{-n}$; Y_0 is a parameter of the initial immersed constant phase angle element Q_c whose impedance is equal to $Z_{Qc} = 1/Y_0 \bullet (j\omega)^{-n}$; The relative permittivity of water ε_w is about 80 [21].

The analysis shows that when the appropriate amount of nano-silica is added to the epoxy resin matrix, a "core-shell transition layer" structure is formed. The "core" acts as the crosslinking point, which increases the crosslinking degree of the composite material and makes it difficult for the polar groups to orient themselves, thus decreasing the dielectric constant of the epoxy resin coating. Dielectric constant is a key indicator reflecting the polarization and charge storage capability of dielectrics, and is closely related to coating impedance. Under an alternating electric field, the coating can be equivalent to a parallel-plate capacitor. A higher dielectric constant corresponds to a larger capacitance and lower system impedance, while a lower dielectric constant results in higher impedance. In nano-SiO_2 modified epoxy coatings, properly dispersed nano-silica fills voids and defects through physical packing and interfacial interactions, forming a dense organic-inorganic hybrid structure, which reduces the dielectric constant and significantly improves the electrochemical impedance. Overloading of nano-SiO_2 leads to particle agglomeration, interfacial defects and stress concentration, accelerating the diffusion of corrosive media, thus increasing the dielectric constant, reducing the impedance and weakening the anti-corrosion performance. The radius of the impedance arc in electrochemical impedance spectroscopy is positively related to the coating impedance, which directly reflects the protective performance. With the addition of an appropriate amount of nano-SiO_2, the dielectric constant of the coating decreases and the radius of the impedance arc increases obviously, indicating improved compactness and barrier property. Excessive nano-SiO_2 causes agglomeration and internal defects, increasing the dielectric constant and reducing the impedance and protection efficiency. Therefore, adjusting the content of nano-SiO_2 can optimize the dielectric constant and impedance, thereby enhancing the corrosion resistance of epoxy coatings.

Figure 12 shows the volume fraction of water absorbed by MES4. Equation (2) is accurate when the coating metal substrate has not undergone corrosion. Therefore, the early water absorption volume fraction of MES4 was studied. The penetration rate of water in MES4 was relatively slow. Following a 30-hour immersion in a 3.5 wt.% NaCl solution, the water absorption volume fraction for MES4 rose to just 23.7 %. The results demonstrate that incorporating hydrophobic nano-silica nanoparticles effectively delays diffusion of corrosive media. This enhancement occurs by improving water resistance in the coating.

https://doi.org/10.64486/m.66.1.7

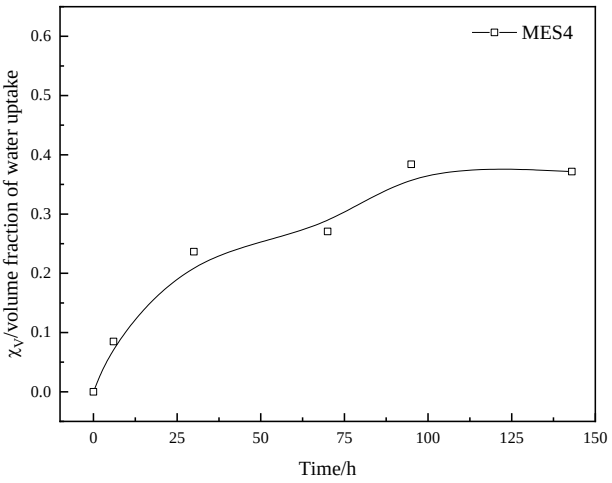

Figure 12. Water absorption volume fraction of MES4

Figure 13 depicts the corrosion characteristics of carbon steel with different coatings in a 3.5 wt.% NaCl solution across various immersion durations. After 24 h immersion, TES, MES1, and MES2 exhibited significant corrosion. The surfaces yellowed, indicating iron hydroxide formation. Blisters formed on MES1 and MES2 after 24 h. In contrast, MES3 and MES4 surfaces showed minimal change. At 168 h, TES, MES1, and MES2 coatings displayed severe corrosion. MES3 and MES4 had only a few microbubbles, indicating superior corrosion resistance. After 336 h, TES, MES1, and MES2 were nearly destroyed with heavy corrosion deposits. However, MES3 and MES4 showed no obvious corrosion products but minor blisters. Additionally, Figure 13 also indicates that MES4 with hydrophobic nano-silica provided the best corrosion resistance.

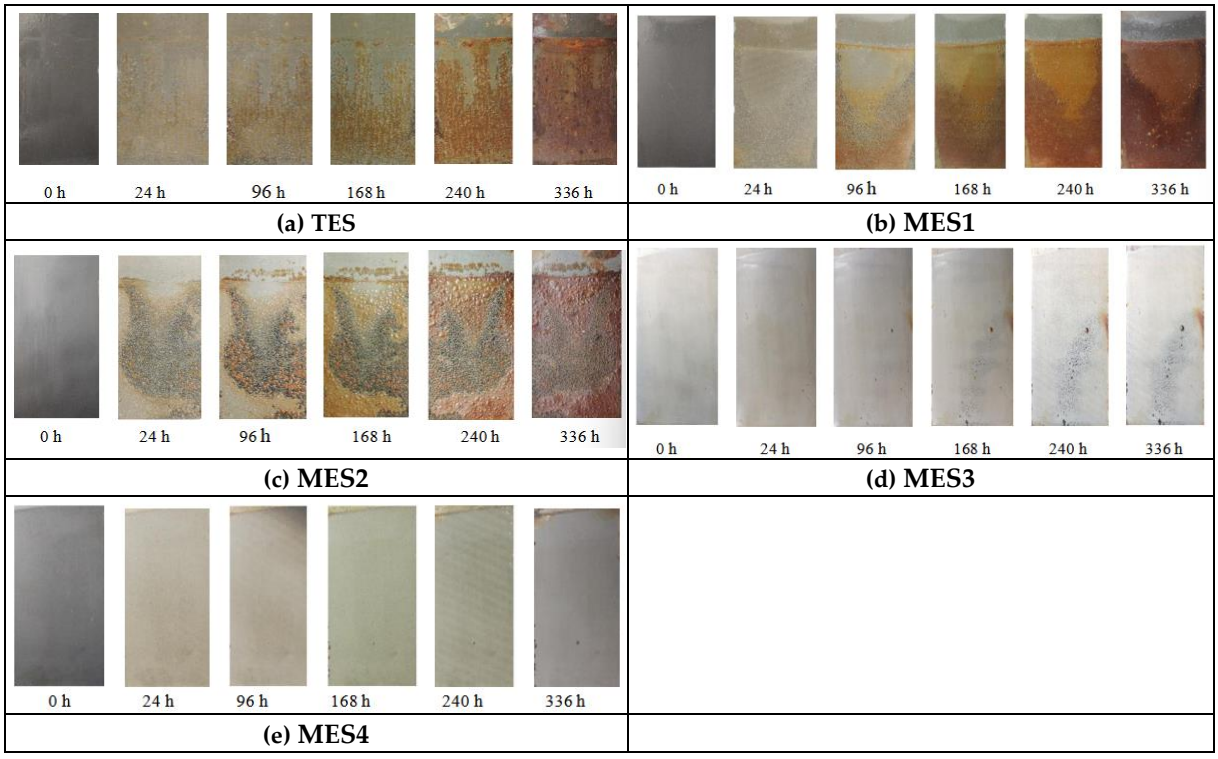

Figure 13. Carbon steel of TES(a), MES1(b), MES2(c), MES3(d) and MES4(e) immersed in 3.5 wt.% NaCl aqueous solution for different times

https://doi.org/10.64486/m.66.1.7

4.1.5 The corrosion protection mechanism

Based on the above results, nano-silica can enhance the corrosion resistance of epoxy resin coatings. The enhanced corrosion resistance of epoxy coatings incorporated with hydrophobic nano-silica can be explained by multiple synergistic mechanisms. First, nano-silica particles fill microvoids and cracks in the epoxy matrix, densify the coating structure, and extend the diffusion path of corrosive media such as water and ions, thereby strengthening the physical barrier effect. Second, hydrophobic nano-silica increases surface water contact angle and reduces water wettability, inhibiting the intrusion of aqueous corrosive substances. Third, the nanoparticles improve interfacial adhesion between the coating and phosphated Q235 steel via mechanical interlocking and interfacial interactions. These effects jointly block electrochemical corrosion pathways, suppress anodic and cathodic reactions, and significantly improve protective performance.

5. Conclusion

Hydrophobic nano-silica-modified epoxy coatings were prepared and characterized by microscopic morphology, wettability, thermal stability, and corrosion behavior. Key findings include:

(1) Higher nano-silica content increased aggregate formation, theoretically enhancing corrosion resistance.

(2) Addition of hydrophobic nano-silica improved thermal stability; MES3 exhibited the highest residual mass, approximately 27 % at 450 °C, which can be attributed to its higher nano-silica content and improved coating compactness.

(3) Elevated nano-silica content raised water contact angles, with MES4 reaching 95.9°, confirming hydrophobicity.

(4) Increased impedance with higher silica addition indicated better anticorrosion performance, attributed to extended diffusion paths and delayed water diffusion.

The study confirmed that hydrophobic nano-silica doping significantly enhances the corrosion resistance of epoxy coatings, as confirmed by corrosion tests. A limitation was the non-uniform dispersion of nano-silica particles in the prepolymer. Future research should optimize dispersion processes to address this weakness and improve coating performance for industrial applications.

Acknowledgments

This work was financially supported by Hebei Province '333 Talent Project' Funding Program: Preparation of Functional Composite Epoxy Resin Coating and Its Corrosion Resistance (No. A202101107) and Tangshan University PhD Innovation Fund project (No. BC202112).

References

[1] K. T. Sun, W. C. Zhong, S. Q. Huang, et al., "Research Progress on the Corrosion Mechanism and Protection Monitoring of Metal in Power Equipment," *Coatings*, vol. 15, no. 2, Art. no. 119, 2025, https://doi.org/10.3390/coatings15020119

[2] J. Tan, L. Liu, H. Wang, et al., "Advances in anti-corrosion coatings on magnesium alloys and their preparation methods," *Journal of Coatings Technology and Research*, vol. 21, pp. 811–825, 2024, https://doi.org/10.1007/s11998-023-00887-z

[3] J. J. Cai , X. Zhang, Z. Wang, et al., "A bio-based antibacterial epoxy resin coating with outstanding flame retardant and mechanical properties," *Progress in Organic Coatings*, vol. 190, Art. no. 108369, 2024, https://doi.org/10.1016/j.porgcoat.2024.108369

[4] M. Toozandehjani, P. M. Nia, E. A, Lotf, et al., "Aluminum Composite Powder as an Additive in Epoxy Coatings for Enhancement of Corrosion Protection of Carbon Steel," *Journal of Central South University*, vol. 31, no. 3, pp. 723–736, 2024, https://doi.org/10.1007/s11771-024-5596-5

https://doi.org/10.64486/m.66.1.7

[5] L. Xu, X. Yang, X. Fu, et al., "Fluorinated Epoxy Based Superhydrophobic Coating with Robust Self-healing and Anticorrosive Performances", *Progress in Organic Coatings*, vol. 171, pp. 107045, 2022, https://doi.org/10.1016/j.porgcoat.2022.107045

[6] W. L. Fu, S. N. Shi, J. Ge, et al., "Research Progress of Anti-corrosion Fillers for Epoxy Coating," *Modern Chemical Industry*, vol. 40, no. 5, pp. 56–62, 2020, https://doi.org/10.16606/j.cnki.issn0253-4320.2020.05.013

[7] O. Grari, A. E. Taouil, L. Dhouibi, et al., "Multilayered Polypyrrole – SiO_2 Composite Coatings for Functionalization of Stainless Steel: Characterization and corrosion protection behavior," *Progress in Organic Coatings*, vol. 88, pp. 48–53, 2015, https://doi.org/10.1016/j.porgcoat.2015.06.019

[8] S. Shi, Y. Zhao, Z. Zhang, et al., "Corrosion Protection of A Novel SiO_2@PANI Coating for Q235 Carbon Steel," *Progress in Organic Coatings*, vol. 132, pp. 227–234, 2019, https://doi.org/10.1016/j.porgcoat.2019.03.040

[9] R. N. Peres, E. S. F. Cardoso, M. F. Montemor, et al., "Influence of the Addition of SiO_2 Nanoparticles to a Hybrid Coating Applied on an AZ31 Alloy for Early Corrosion Protection," *Surface and Coatings Technology*, vol. 303, pp. 372–384, 2016, https://doi.org/10.1016/j.surfcoat.2015.12.049

[10] H. Guo, C. Yang, H. Sun, et al., "TEOS-modified SiC Superhydrophobic Nanostructures in Epoxy Resin Coatings for Corrosion Prevention," *Surface and Interfaces*, vol. 46, Art. no. 104057, 2024, https://doi.org/10.1016/j.surfin.2024.104057

[11] J. Fan, Z. Long, J. Wu, et al., "Electrothermal Superhydrophobic Epoxy Nanocomposite Coating for Antiicing/deicing," *Journal of Coatings Technology and Research*, vol. 20, no. 5, pp. 1557–1568, 2023, https://doi.org/10.1007/s11998-023-00762-x

[12] S. C. Yuan, Y. Sun, C. Yang, et al., "A Novel Dual-functional Epoxy-based Composite Coating with Exceptional Anti-corrosion and Enhanced Hydrogen Gas Barrier Properties," *Chemical Engineering Journal*, vol. 449, Art. no. 137876, 2022, https://doi.org/10.1016/j.cej.2022.137876

[13] H. Liu, S. Szunerits, W. Xu, et al., "Preparation of Superhydrophobic Coatings on Zinc as Effective Corrosion Barriers," *ACS Applied Materials & Interfaces*, vol. 1, no. 6, pp. 1150–1153, 2009, https://doi.org/10.1021/am900100q

[14] F. Zhang, S. Chen, L. Dong, et al., "Preparation of Superhydrophobic Films on Titanium as Effective Corrosion Barriers," *Applied Surface Science*, vol. 257, no. 7, pp. 2587–2591, 2011, https://doi.org/10.1016/j.apsusc.2010.10.027

[15] X. F. Zhang, X. D. Li, N. Wang, et al., "Robust Superhydrophobic SiO_2/Epoxy Composite Coating Prepared by One-step Spraying Method for Corrosion Protection of Aluminum Alloy: Experimental and Theoretical Studies," *Materials & Design*, vol. 228, Art. no. 111833, 2023, https://doi.org/10.1016/j.matdes.2023.111833

[16] C. Yang, X. D. Tang, J. J. Li, et al., "Synthesis Technology Progress of Bisphenol A Epoxy Resin," *China Plastics*, vol. 37, no. 2, pp. 106-112, 2023, https://doi.org/10.19491/j.issn.1001-9278.2023.02.015

[17] J. P. Wang, W. J. Qu, Y. N. Lei, et al., "Preparation and Anti-corrosion Performance Research of Epoxy/Nano-silica Composite Coating," *Electroplating and Finishing*, vol. 39, no. 6, pp. 299–305, 2020, https://doi.org/10.19289/j.1004-227x.2020.06.001

[18] L. Ejenstam, L. Ovaskainen, I. Rodriguez-Meizoso, et al., "The Effect of Superhydrophobic Wetting State on Corrosion Protection-The AKD Example," *Journal of Colloid and Interface Science*, vol. 412, pp. 56–64, 2013, https://doi.org/10.1016/j.jcis.2013.09.006

[19] B. Ramezanzadeh, S. Niroumandrad, A. Ahmadi, et al., "Enhancement of Barrier and Corrosion Protection Performance of an Epoxy Coating Through Wet Transfer of Amino Functionalized Graphene Oxide," *Corrosion Science*, vol. 103, pp. 283–304, 2016, https://doi.org/10.1016/j.corsci.2015.11.033

[20] D. N. Dang, B. Peraudeau, S. Cohendoz, et al., "Effect of Mechanical Stresses on Epoxy Coating Ageing Approached by Electrochemical Impedance Spectroscopy Measurements," *Electrochimica Acta*, vol.124, pp. 80–89, 2014, https://doi.org/10.1016/j.electacta.2013.08.111

[21] P. Z. Gao, M. Q. Lin, H. J. Lin, et al., "Research on the Properties of Nano-silica Modified Epoxy Composites," *Journal of Hunan University (Natural Science Edition)*, vol. 42, no. 6, pp. 1–6, 2015, https://doi.org/10.16339/j.cnki.hdxbzkb.2015.06.001

https://doi.org/10.64486/m.66.1.7